LSST's Plans for Calibrated Photometry

Robert Lupton, Mario Jurić, and Christopher Stubbs

February 12, 2016

Contents

1 Introduction

In addition to photometry LSST needs to worry about calibrating astrometry and the PSF, but these topics are not covered here.

In the notation defined in "Level 2 Photometric Calibration for the LSST Survey" Jones et al. 2013. the number of detected counts (*i.e.* DN) $C_{raw,b}$ from an astronomical source with flux F_ν in time Δt in band b is

$$C_{raw,b} = \frac{\pi D^2 \Delta t}{4gh} \int_0^\infty F_\nu(\lambda) S^{atm}(\lambda) S_b^{sys}(\lambda)\, d\lambda/\lambda$$

where D is the telescope's effective diameter, g the gain (photoelectrons per DN), and h Planck's constant. The term 'detected' is taken to mean those photons which are measured as part of the PSF, as opposed to those spread out over the focal plane by scattering and ghosting.

We are interested in S^{atm} and S_b^{sys}, the probabilities of a photon passing through the atmosphere and telescope/camera (including the mirrors, filter, and lenses) and being detected. We shall also need $S_{b,std}$, which we shall choose to be close to an average $S^{atm} S_b^{sys}$, probably at an airmass of *c.* 1.2.

Our task is, of course, to estimate $C_{std,b} \equiv \int_0^\infty F_\nu S_{b,std}\, d\lambda/\lambda$ given $C_{raw,b}$; doing this correctly requires knowledge of the object's SED.

Measuring $C_{std,b}$ splits into a number of separate operations, and we need to estimate:

- the detector sensitivity $S_b^{sys}(\lambda, \boldsymbol{x})$, including
  - the atmospheric transmissivity $S^{atm}(\lambda)$
  - the telescope (including optics and filters)
  - the detector efficiencies
- the object's SED
- the background level and $C_{raw,b}$

1.1 Absolute Photometry

This document is written assuming that we can generate absolute photometry tied to NIST-certified photo-diodes. We accept that this is a radical and unproven approach, and in reality we will need externally defined standards in order to either establish or validate our photometry.

One obvious possibility is dA white dwarfs, whose atmospheres (and circumstellar dust) are thought to be understood at the 1-3% level.

Another possibility that is at least amusing is to use SNe Ia's at a redshift where the cosmology is reliably measured using BAOs ($a \approx 0.7$?); we would then use SNe Ia's at lower redshift to fill out the Hubble diagram.

We defer a careful discussion of this issue to a later revision of this document.

2 The instrumental sensitivity $S_b^{sys}(\lambda, \boldsymbol{x})$

Measuring $S_b^{sys}(\lambda, \boldsymbol{x})$ requires us to measure the variation with $\boldsymbol{x}$ (the flatfield) and with λ (the effective filter bandpass); these two effects are not really separable. We must also ask what we mean by 'effective filter bandpass':

A number of data sets are available to measure the *in situ* sensitivity:

- Broad-band dome flats
- "Monochromatic" (*c.* 1nm bandwidth) flats, calibrated with NIST photodiodes observing the calibration screen.
- Dithered star fields
- A set of spots from the collimated projector (see Appendix A).

Let $\mathcal{I}(\lambda, \boldsymbol{x})$ be the illumination of the focal plane due to the illuminated flatfield screen in the absence of telescope and filter effects; we know the wavelength dependence of the screen illumination from the NIST diode data.

You might hope that $\mathcal{I}$ would be a function only of λ and the flatfield image $\mathcal{F}_b(\lambda, \boldsymbol{i})$ would simply be to $\mathcal{I}(\lambda)\, S_b^{sys}$; unfortunately your hopes are unfounded.

If the flatfield screen were at infinity, there was no vignetting, and the screen were perfectly Lambertian, then non-uniform illumination of the dome screen would have no effect on the uniformity of $\mathcal{I}$; in reality these conditions are not all met and the illumination becomes $\mathcal{I}_0 + i(\lambda, \boldsymbol{i})$.

$\mathcal{F}_b$ also includes scattered light and ghosting (the latter a strong function of wavelength due to the details of the filter b's transmission function) so we must split $\mathcal{F}_b$ into multiplicative and additive parts:

$$\mathcal{F}_b(\lambda, \boldsymbol{i}) \equiv I(\lambda)\,(1 + i(\lambda, \boldsymbol{i}) + \mathcal{A}_b(\lambda, \boldsymbol{i}))\,\mathcal{S}_b(\lambda, \boldsymbol{i})$$

(assuming that the dome is light-tight and contains no glowing LEDs, in other words that $\mathcal{F}$ is proportional to the illumination level). We wrote $\mathcal{S}_b$ not S_b^{sys} because there are multiplicative effects (*e.g.* pixel size variations) other than quantum efficiency that enter into $\mathcal{F}_b$, and which are included in $\mathcal{S}_b$.

We expect the $\mathcal{A}_b$ term to be a strong function of wavelength as reflections off the filter are a significant contribution to the ghosts*

We propose an approach to disentangling these effects in section 2.3, and shall discuss how to harness our knowledge of $\mathcal{A}$ and $\mathcal{S}$ in sections 4 and 6.

2.1 Multiplicative Effects

Structures seen in $\mathcal{S}_b$ can come from either QE variations in the system (*e.g.* dust on the filter or surface annealing modulating the detector's sensitivity) and vignetting†, or changes in the effective size of the pixels:

$$\mathcal{S}_b(\lambda, \boldsymbol{i}) = \mathcal{S}_b^{filt}(\lambda, \boldsymbol{i}) \times \mathcal{S}^{tel}(\lambda, \boldsymbol{i}) \times \mathcal{S}^{vig}(\lambda, \boldsymbol{i}) \times \mathcal{S}^{qe}(\lambda, \boldsymbol{i}) \times \mathcal{S}^{geom}(\lambda, \boldsymbol{i})$$

* if the filter transmission is $T(\lambda)$, the intensity that is reflected once and transmitted once is of course $T(1-T)$ and reaches 25% at the 50% point at the edge of the bandpass.

† The effects of vignetting and QE variation cannot be separated if we're considering light from the entire pupil as both lead to lost photons; in the former case because they never reach the focal plane and in the latter because the photon isn't absorbed by the detector. This degeneracy is broken when we consider the collimated projector in section 2.3

We may further split the 'geom' part into optical distortion and CCD effects such as "tree-rings" or mask step errors:

$$= \mathcal{S}_b^{filt}(\lambda, \boldsymbol{i}) \times \mathcal{S}^{tel}(\lambda, \boldsymbol{i}) \times \mathcal{S}^{vig}(\lambda, \boldsymbol{i}) \times \mathcal{S}^{qe}(\lambda, \boldsymbol{i}) \times \mathcal{S}^{optics}(\lambda, \boldsymbol{i}) \times \mathcal{S}^{ccd}(\lambda, \boldsymbol{i})$$

The last three terms are only a weak (or very weak) function of wavelength; they can vary due to chromatic optical distortions and *e.g.* variations in the importance of detector effects with conversion depth.

For measures of surface brightness QE/vignetting and geometrical effects are equivalent, but for measurements of objects' fluxes we must be careful to separate them; treating larger pixels as more sensitive can give incorrect results.*

The camera team will provide enough information to determine $\mathcal{S}^{ccd}$; the details are *T.B.D.*. The $\mathcal{S}^{optics}$ part will initially come from the optical design, but in production will come from the astrometric solution which will determine it with exquisite precision. We only need to know $\mathcal{S}^{vig}$ in order to make an *ab initio* model of the system, and to estimate the importance of non-uniform illumination of the flatfield screen.†

2.2 Using Star Flats

The classical solution to this problem is to take the dome flat at face value as a measure of quantum efficiency, then take a number of exposures of a star field at a set of boresight offsets, flatfielding using our dome-based flat fields. If we make the reasonable assumption that most of the stars are not variables, we may setup and solve a system of linear equations for a model of a reasonably slowly varying correction to the domeflat — the illumination correction — and also the brightnesses of all the stars (here just a set of nuisance parameters); the combination of this illumination correction and the domeflat is $S_b^{sys}(\lambda, \boldsymbol{i})$.

Because we are interested in the effects of objects' SED on their photometry we would have to generalise this to make use of the colours of the stars. It seems possible that this would enable us to measure the wavelength dependence of the spatial structure of the illumination correction well enough to produce reliable colours for stars and normal galaxies, but it's improbable that the diversity of star colours is large enough to measure it well enough to handle an arbitrary SED.

2.3 Using the Collimated Projector

As discussed in Appendix A, we will be able to project a mask with a set of holes onto the focal plane. Each hole produces a *c.* 50pixel spot‡ and a series of ghosts; the density of holes in the mask will be chosen to allow us to separate the primary spots from the ghosts, possibly using an optical model of the system. In the discussion of $\mathcal{F}$ above we implicitly defined the system throughput to be the fraction of the incident light that is detected in the primary spot, with the ghosts creating $\mathcal{A}$.

Because our projector only illuminates a small portion of the primary we need to extend our notation (and writing $\mathcal{S}^{tel,vig} \equiv \mathcal{S}^{tel}\mathcal{S}^{vig}$):

$$\mathcal{F}_b(\lambda, \boldsymbol{i}) \equiv I\, \mathcal{S}^{qe,optics,ccd} \int_{pupil} (1 + i + \mathcal{A}_b)\, \mathcal{S}_b^{filt} \mathcal{S}^{tel,vig}\, d\boldsymbol{X}$$

*Flux is conserved, so if we are making a measurement of flux ignoring pixel size variation gives the correct result for all pixels which are given the same weight (*e.g.* pixels entirely included in the aperture)

† We also theoretically need it to measure the filter profiles using a widget such as that mentioned in a footnote in section 2.5.

‡Available projectors are close to diffraction limited, and with a 30cm diameter we should be able to produce images as small as 0.7" FWHM at $1\mu m$.

Note that an integral over the pupil is automatically an integral over photon arrival directions. We are assuming that *e.g.* the effective size of the pixel isn't a function of the incident angle of the photon, which seems likely to be very nearly true (although this assumption isn't fundamental).

We may write the total flux in the primary image of the ℓ^{th} spot imaged through the b filter in a narrow range around wavelength λ at the point $\boldsymbol{x}_i$ as

$$P_b^\ell(\lambda, \boldsymbol{x}_i, \boldsymbol{X}) = a^\ell I(\lambda)\,(1 + i(\lambda))\mathcal{S}_b^{filt}(\lambda)\mathcal{S}^{tel,qe,vig,optics,ccd}(\lambda)$$

and, if we take a series of exposures that collectively illuminate the entire primary (and dropping the explicit λ for readability) we may evaluate

$$P_b^\ell(\boldsymbol{x}_i) = a^\ell I\,\mathcal{S}^{qe,optics,ccd}\int_{pupil}(1 + i)\mathcal{S}_b^{filt}\mathcal{S}^{tel,vig}\,d\boldsymbol{X}$$

At this point we know the relative spectral response at a set of points in the focal plane.

If we now move these spots around the LSST focal plane, taking data at only a single position in the pupil and wavelength, we may solve for the relative sensitivities between the spots $\{\ell\}$ in a manor exactly equivalent to star-flat approach of section 2.2.* We would repeat this analysis at a (sparse) set of wavelengths to check for chromatic effects in the hole's throughputs due to *e.g.* diffractive effects

Once we know the a^ℓ's, we scale all the spot intensities to a common scale,

$$P_b^\ell(\boldsymbol{x}_i) = I\,\mathcal{S}^{qe,optics,ccd}\int_{pupil}(1 + i)\mathcal{S}_b^{filt}\mathcal{S}^{tel,vig}\,d\boldsymbol{X}$$

and

$$\mathcal{F}_b(\lambda, \boldsymbol{x}_i) = P_b^\ell(\boldsymbol{x}_i) + I\,\mathcal{S}^{qe,optics,ccd}\int_{pupil}\mathcal{A}_b\mathcal{S}_b^{filt}\mathcal{S}^{tel,vig}\,d\boldsymbol{X}$$

If, as would be expected, the first term varies only slowly over a chip, then rastering the spots to illuminate some number *T.B.D.* of positions on each chip allows us to $P_b^\ell(\boldsymbol{i})$, *i.e.* at every pixel. Unfortunately we still don't know how to find the pixel-to-pixel variability. If there is a clear separation between the spatial scales probed by P and $\mathcal{F}$ (*i.e.* and $\mathcal{A}$) we can combine the two estimates to generate a flatfield uncontaminated by scattered light and ghosting.

For many cameras the spatial structure of $\mathcal{A}$ has sharp features. Furthermore, the operations described above are expensive (see Table 2), and we have to repeat for every *c.* 1nm step in wavelength. If we know the filter bandpasses $\mathcal{S}_b^{filt}(\boldsymbol{i})$ at every point in the focal plane (see section 2.5) we may use a slightly different approach.

If we take both domeflat and collimated projector data without a filter in the beam† we may repeat the above analysis without the $\mathcal{S}_b^{filt}$. This has two advantages: there are no strongly chromatic elements so we can use larger steps in wavelength; and the $\mathcal{A}$ image should be much weaker (as much of it comes from the filter edges). Having **XXX achieved a separation of scales**, we have measured $\mathcal{S}^{qe,optics,ccd,tel,vig}(\lambda, \boldsymbol{i})$ and knowing $\mathcal{S}_b^{filt}(\lambda, \boldsymbol{i})$ we have measured our desired sensitivity with only one remaining contaminant: the non-uniform illumination resulting from an imperfect flatfield screen, i (see next section).

* This rasterisation is a little tricky. If we simply tilt the projector to move the spots they will illuminate a different part of the primary; if also move the projector we can arrange that the footprint on one of the optical elements (primary, secondary, filter, ...) remains fixed. As an alternative we can move the mask relative to the projector's optic axis and adjust the projector to keep the spots fixed; we can then solve for the variation of brightness around the projector's focal plane. If this is stable we can then translate the mask when determining the individual holes' throughputs. In reality we would do both.

† The projector beam is so slow that the image quality should not be significantly degraded

2.3.1 Characterising the Ghosts

We have worked hard to avoid contaminating our $\mathcal{S}$ estimates with ghosts and scattered light, but we can now carry out a consistency check. In addition to the $P_b^\ell(\lambda)$ we can **XXX probably** measure the ghosts, $G_b^\ell(\lambda)$. By interpolating and then summing over the focal plane we have an estimate of $\mathcal{A}_b$; it will be interesting to see how well this works.

2.4 Non-uniform Dome Flat Illumination, i

Because the screen isn't at infinity and because of vignetting, surface brightness variation over the flat field screen leads to spatial structure in the focal plane: $i \neq 0$.

We may get a handle on this surface brightness by employing a pinhole camera in place of a filter. **XXX Chris Stubbs worries that the angular distribution of light imaged by this camera is very different from the domeflat illumination; *c.* $f/1$ as opposed to only within 1.75° of normal. which would require us to know the screen's BDRF to make appropriate corrections. I don't see this, as the pinhole is in the same beam** Alternatively, we expect the effects of i to be have only weak spatial and spectral variability. If this is the case, we can use dithered star fields to make a correction.

2.5 Measuring the Filter Profiles

We may have lab measurements of the filter profiles at a dense grid of points over the filters.*

Alternatively the unfiltered data also allows us to measure (or monitor) the filter bandpasses. As mentioned above, scanning a spot in wavelength measures the sensitivity of a point in the focal plane, so the ratio of the sensitivity measured with and without the filter is the filter bandpass:

$$\frac{P_b^\ell}{P_{clear}^\ell} = \frac{\int_{pupil}(1+i)\mathcal{S}_b^{filt}\mathcal{S}^{tel,vig}\,d\boldsymbol{X}}{\int_{pupil}(1+i)\mathcal{S}_{clear}^{filt}\mathcal{S}^{tel,vig}\,d\boldsymbol{X}}$$

(again assuming that $\mathcal{S}^{qe,optics,ccd}$ are not dependent on λ). If i is well behaved (*e.g.* Lambertian) this is exactly what we want, with the correct average over the rays traversing the filter.

2.5.1 Fringing

There is one extra wrinkle. CCDs behave like Fabry-Perot cavities, and this modulates the throughput. Because the spatial variability comes from thickness variations in the devices it can have fine scale structure, and the correct way to measure this is with a white-light flat-field exposure taken at *c.* 1nm spacings. We include an estimate of how long it would take to acquire this data in Section B, but it is not obvious if this is really necessary.

Fringing in the LSST chips is expected to be small as not only are the devices thick, so little light is returned from the bottom of the device to interfere, but also the very fast beam washes out the effect. Preliminary estimates (Rasmussen 2015) suggest that fringing will not be important for LSST, but we believe that it would be premature to ignore its effects. Note that fringing is important even in the absence of strong emission lines; lines produce clear artifacts in the sky brightness, but interference modulates the sensitivity even for continuum sources.

* For example by scanning an beam with the appropriate range of f-ratios to simulate the LSST beam across the filter and collecting the transmitted light into a spectrophotometer

3 The atmospheric transmissivity $S^{atm}(\lambda)$

The current baseline plan is to use a 1.2m telescope with $R \sim 300$ — 400 to take spectra of standard stars with a cadence of *c.* 5 minutes (3 minutes to integrate; 2 minutes to slew and acquire). The expected S/N at 12^{th} magnitude is 500/resolution element (300 in u and y).

There will also be two units to measure water vapour; a all-sky monitor using GPS satellites and a bore-sight mounted radiometer to measure the vertical profile.

The baseline proposal is to use these spectra to find the atmospheric absorption along the line of sight to standard stars (*n.b.* with a inter-visit time of 5 minutes there will be *c.* one exposure per 10 LSST visits). We will then decompose the atmospheric transmission into a set of basis functions and use these to interpolate in space and time to find S^{atm} at any position in the focal plane.

The task of reducing these data has two phases:

- Generate calibration products sufficient to extract accurate spectrophotometry from 2-d spectra **XXX What these are needs to be sorted out; do we need a monochromater in addition to quartz and arc lamps?**

- Define n components which describe S^{atm}. These could come either from from MODTRAN (with modified aerosol absorption properties estimated from the data) or a PCA-like decomposition of all the data we've already taken. This latter choice is not able to detect a constant (but chromatic) component – we're only sensitive to the variation in the atmospheric properties. This decomposition must be able to interpolate in airmass over a limited range (the scale is between half the LSST focal plane and *c.* 3 times larger if the auxiliary telescope cadence is 10 times slower than the main telescope).

- Acquire "ground truth" spectro-photometric spectra for all stars that will be observed by the auxiliary telescope. *e.g.* Using the auxiliary telescope, booststrap from dA white dwarfs with known SEDs **XXX Are WD SEDs really known well enough? 1-2%?**. *n.b.* Again, we could bootstrap these SEDs from the data given enough observations, subject to an overall constant chromatic scaling; this seems much scarier than determining the atmospheric components from the data.

Then, for each exposure,

- Remove the instrumental signature from the 2-d data.

- Extract a wavelength and intensity calibrated 1-d spectrum, presumably using a 1-d 'optimal' extraction algorithm.

- Given the known spectrum of the object and the extracted spectrum, fit the parameters describing the atmosphere.

n.b. we would probably really combine these two steps and directly fit for the atmospheric parameters given the post-ISR 2-d data

XXX It is a non-trivial task 'Extract a wavelength and intensity calibrated 1-d spectrum'

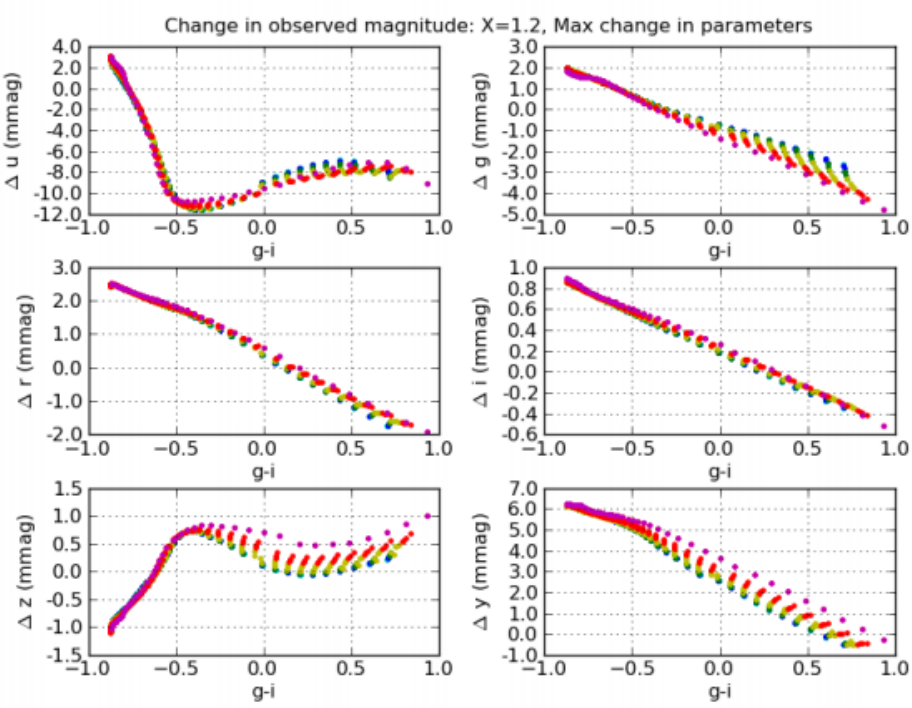

Figure 1: The change in the observed magnitude of stars in the temperature range 5000—35000K as the properties of the atmosphere are changed between two extreme models, keeping the airmass fixed at 1.2. The different coloured points correspond to a range of metallicity and gravity.

3.1 Required S/N

The base-line plan expects a S/N of 300 — 500 per resolution element for a **XXX 180s** integration on a 12^{th} magnitude star, with $R \sim 400$ (a total S/N of *c.* 6000 — 10000). This will be used to determine *c.* 6 parameters describing the atmospheric transmission.

Apart from the overall cloud extinction (a serious problem with which this telescope does not help), these numbers will result in corrections of at most 3%, so we need to know them in turn to 3% to achieve 1mmag photometry, *i.e.* an S/N of *c.* 30; with 6 parameters we need a total S/N of *c.* 200 which can be achieved in *c.* 7s for a 12^{th} magnitude object. Alternatively, given a 180s exposure we can use stars as faint as 15.5.

The overhead between exposures is currently thought to be **XXX 120s**, so there's no point going significantly below a 60s exposure unless we can build a more agile auxiliary telescope.

3.2 Stellar Photometry

To determine the optimal use of auxiliary data we need to see what can be learned directly from the photometry and what information must come from elsewhere.

We will have many-colour photometry (*ugrizy*) of **XXX many, many** stars in each visit. We know from simulations of Kurucz models that as the properties of the atmosphere are varied there are several percent level changes in fluxes, with percent-level scatter at a given $g - i$ colour (See figure 1). It is not yet clear how much of this scatter can be regressed out using all five available colours (see also section 5). If the conditions are not photometric this is not an insuperable problem as the positions of red and blue stars do not correlate with the regions of dense cloud — but it does make it harder. If the structure of the extinction is sufficiently complex we will not be able to

reach SRD precision independent of our ability to correct for the subtle effects of the atmosphere.

Even if the scatter can be removed to SRD precision (see appendix C), it is not clear how well we will be able to characterize S^{atm} across the filter b. In reality the solution should use all available information (*e.g.* satellite-based ozone; atmospheric pressure; water-vapour).

XXX We need to do a study on way of characterising the atmosphere. Probably the i-band is the most interesting as it is subject to effects from aerosols (two parameters), water vapour (one), and XXX Rayleigh scattering (one).

3.3 Spatial Structure of the Atmosphere

Even if the photometry is unable to constrain S^{atm} well enough to satisfy the SRD requirements, it seems very likely that we will be able to say something interesting. Once we have implemented an initial version of the photometric analysis we will be able to analyse wide-field camera data to explore the structure functions. Obvious candidates are SDSS stripe82, DECam, and HSC. These cameras have obvious tradeoffs in data availability, available integration times, maximum scale probed and object density (and hence spatial resolution).

4 Flatfields

Section 2 discusses analysing the response to the flatfield screen, $(1 + i + \mathcal{A}_b)\mathcal{S}_b^{filt}\mathcal{S}^{tel}\mathcal{S}^{qe}\mathcal{S}^{optics}\mathcal{S}^{ccd}$. Before we can create a flatfield image for band b we need to:

- Decide what to do about $i(\lambda, \boldsymbol{i})$
- Decide what to do about $\mathcal{A}_b(\lambda, \boldsymbol{i})$
- Decide what to do about $\mathcal{S}^{optics}(\lambda, \boldsymbol{i})$
- Decide what to do about $\mathcal{S}^{ccd}(\lambda, \boldsymbol{i})$
- Choose an SED

Correcting for i is always desireable and we shall assume that it's been accomplished.* It might seem obvious that the flatfield should exclude $\mathcal{A}$ and correct for $\mathcal{S}^{optics}\mathcal{S}^{ccd}$, resulting in a map of the detector's true QE. However, this is probably not a good idea as it

- leads to a complex background image
- does not remove the need for sufficiently scrupulous algorithms to require access to the per-pixel geometrical information.

Once the data is warped to *e.g.* a tangent plane these geometrical effects on QE are removed (the resampling kernels include the determinant of the transformation's Jacobian).† It would be possible to remove the effects of the dimensions of individual pixels at the same time, but we shall choose to forgo this option; see the discussion of background estimation in section 6.

Removing $\mathcal{A}_b$ from the flatfield also complicates the background, adding the scattered light and ghosting back into the data. As background estimation is already a challenging task (even with background matching), this seems undesirable.

We therefore propose that the flatfields be calculated as follows:

*A better solution would be to design a flatfield screen which delivers $i \equiv 1$

† The inevitable distortion of the new projection will of course lead to a new $\mathcal{S}_b^{optics}$.

- Use the sky's SED modified by $\mathcal{S}_b^{filt}$. We could use different sky models for different phases of the moon (or solar cycle), or measure the sky emission directly (possibly using the calibration telescope). We will need to at least allow for the phase of the Moon.
- Do not correct for $\mathcal{A}_b$ (resulting in an incorrect estimate of the sensitivity).
- Correct for $\mathcal{S}^{tel}\mathcal{S}^{qe}$
- Correct for $\mathcal{S}^{optics}$
- Do not correct for $\mathcal{S}^{ccd}$

This is the flatfield that best flattens the sky once warped onto a tangent plane, at the cost of photometric errors. We will need to include fringe frames made from medianed sky exposures in the sky model, but the dimensionality of the required fringe set is not yet clear. **XXX Expand at some point**

We will further discuss the consequences of this choice in section 6.

4.1 Flatfields for Level 1

This description is appropriate for level 2 processing, but level 1 is different and we must ensure that the choices made during flatfield generation matches the adopted processing flow. It may turn out that we need different level 1 and level 2 flats.

5 The object's SED

Let us remember that we don't actually need to know the SED; we need merely to know enough about it to allow us to make sufficiently accurate corrections from $C_{raw,b}$ to $C_{std,b}$.

We don't know our objects' SEDs, but we do know their multi-band fluxes $\{C_{std,b}\}^*$ and other parameters θ (*e.g.* morphological information). There is a probability distribution $p(\mathrm{SED}|\{C_{std,b}\},\theta)$ which may be compact, essentially reducing to a single reasonably well-defined SED, or may reflect the intrinsic range of SEDs of objects with those properties.† The parameters θ may include morphology (adopting different SEDs for stars and galaxies), or Galactic (l,b) if we wish to take Galactic reddening into account.

If we restrict our attention to stars, the colours probably determine the SED reasonably well (see section 3.2). Studies of galaxies' photometric redshifts tell us that their SED is often, but not always, reasonably well defined by the colours; QSOs show significant degeneracies, mostly at redshifts below *c.* 2.5.

There is nothing we can do about this degeneracy, which means that we cannot hope to correctly estimate $C_{std,b}$ for a subset of objects which we detect. However, we will need to define a deterministic mapping from colour to $\mathrm{SED}(\{C_b\},\theta)$ which will allow a consumer of the data to make their own correction (see section 6).

If an object appears *ex nihilo* we know nothing about its SED, so we shall have to adopt some spectrum (*e.g.* a flat-spectrum source) and increase the error estimate accordingly. This is unlikely to be important as the SED-based corrections are small.

---

* the distinction between *e.g. std* and *nat* fluxes doesn't really matter here, but if necessary we could iterate the calibration procedure until we arrive at $C_{std,b}$.

† In reality galaxies display colour gradients; we'll return to this in section 6.

6 Measuring the background level and $C_{std,b}$

6.1 Background Subtraction

We plan to background match multiple exposures of a patch of the sky in a given filter before sky subtraction, generating a stacked image in a sky projection.

This results in two data products:

- The background image in the stacked image B^{stack}.
- The differences B^i between this background image and the input images.

Because we measure B^{stack} in sky coordinates the geometrical distortion terms $\mathcal{S}^{optics}$ in the flat-field illumination are automatically removed,* and when we warp B^i back to the corresponding calibrated raw frame and subtract it we arrive at an image with $\mathcal{S}^{optics}$ fully accounted for.

If we had included $\mathcal{S}^{ccd}$ in the flatfield we would have handled the background correctly if we also included it in the warps to and from sky coordinates, but we would not be able to forget about it as it continues to have effects on the astrometry and photometry.†

Having removed the background we can reconsider the choices we took when we built our flatfields (section 4).

- We no longer have any motivation to use the sky's SED (as we have subtracted all the sky photons), but do not know what to use instead to get the correct fluxes for the object photons.
- We should now correct the sensitivity for the effect of $\mathcal{A}_b$ as it no longer complicates the sky subtraction.
- We could decide to now correct for $\mathcal{S}^{ccd}$.

6.2 Measuring $C_{std,b}$

All photometric measurements can be thought of fitting a model M; $I = aM$. Let us take this model to describe the image above the atmosphere, and to be in photons not Joules. We know our object's $(\{C_b\}, \theta)$, so we know which SED we should adopt (section 5).

The signal that we measure after (incorrectly) flat fielding with a flat constructed using the sky's SED is

$$I_j = a \int_b S^{atm}_{obj} \frac{\mathcal{S}^{filt}_{b,j,obj}\mathcal{S}^{tel}_{j,obj}\mathcal{S}^{qe}_{j,obj}}{\mathcal{S}^{filt}_{b,j,sky}\mathcal{S}^{tel}_{j,sky}\mathcal{S}^{qe}_{j,sky}}\mathcal{S}^{ccd}_j M_j P_b(\lambda)\, d\lambda + \epsilon_j \equiv a w_j + \epsilon_j$$

where I_j is the intensity of the j^{th} pixel and ϵ_j the noise. I'll drop the explicit integral over filter b's bandpass P_b so all sensitivities in this section should be taken to be bandpass-averaged.

If we take the ϵ_j to be independent Gaussians $N(0, \sigma_j^2)$, the maximum likelihood estimate for the amplitude a is

$$a = \frac{\sum_j w_j I_j/\sigma_j^2}{\sum_j w_j^2/\sigma_j^2}$$

*They are replaced by $\mathcal{S}^{projection}$, but this term is not dependent on the boresights of the visits.

† it would also have made the warp code more complex and probably slower as the individual area of each pixel would have to be handled explicitly.

and the total number of DN C is $C = a\sum_j w_j$ (this is an unbiased estimate even if the errors aren't Gaussian). It is almost always best to set $\sigma_j^2 = 1$ to avoid systematic errors as a function of magnitude, and we shall do so in this discussion.

Let us assume that the ratios $\mathcal{S}^{filt}_{b,obj}/\mathcal{S}^{filt}_{b,sky}$ $\mathcal{S}^{tel}_{obj}/\mathcal{S}^{tel}_{sky}$ and $\mathcal{S}^{qe}_{obj}/\mathcal{S}^{qe}_{sky}$ are constant for all the pixels in the object. This isn't necessary, we can handle it the same way as we'll handle $\mathcal{S}^{ccd}_j$, but it is probably a good assumption and has some advantages. In this case, we have

$$\begin{aligned} a =& \frac{1}{S^{atm}_{obj}} \frac{\mathcal{S}^{filt}_{b,sky}\mathcal{S}^{qe}_{sky}}{\mathcal{S}^{filt}_{b,obj}\mathcal{S}^{qe}_{obj}} \frac{\sum_j (\mathcal{S}^{ccd}_j M_j) I_j}{\sum_j (\mathcal{S}^{ccd}_j M_j)^2} \\ C =& a \sum_j \mathcal{S}^{ccd}_j M_j \end{aligned}$$

and, correcting to a standard atmosphere, and writing $w = \mathcal{S}^{ccd}_j M_j$

$$\begin{aligned} C_{std} =& \frac{S^{atm}_{obj,std}}{S^{atm}_{obj}} \frac{\mathcal{S}^{filt}_{b,sky}\mathcal{S}^{qe}_{sky}}{\mathcal{S}^{filt}_{b,obj}\mathcal{S}^{qe}_{obj}} \frac{\sum_j w_j I_j \sum_j w_j}{\sum_j (w_j)^2} \\ \equiv& \frac{S^{atm}_{obj,std}}{S^{atm}_{obj}} \frac{\mathcal{S}^{filt}_{b,sky}\mathcal{S}^{qe}_{sky}}{\mathcal{S}^{filt}_{b,obj}\mathcal{S}^{qe}_{obj}} C_{raw} \end{aligned}$$

If we have n exposures this generalises to

$$\begin{aligned} C_{std} =& \sum_r \frac{S^{atm}_{obj,std}}{\mathcal{S}^{atm,r}_{obj}} \frac{\mathcal{S}^{filt,r}_{b,sky}\mathcal{S}^{qe,r}_{sky}}{\mathcal{S}^{filt,r}_{b,obj}\mathcal{S}^{qe,r}_{obj}} C^r_{raw} \\ \equiv& \sum_r c^r_{\rm SED} C^r_{raw} \end{aligned}$$

I have kept the per-visit superscript r in $\mathcal{S}^{filt}$ to allow for spatial variation in the filter properties, and in $\mathcal{S}^{qe}$ to allow for different CCDs in the focal plane having different sensitivities. If you think that the different platescale for object- and sky-coloured objects have a significant effect, you may add the ratio $\mathcal{S}^{tel}_{sky}/\mathcal{S}^{tel}_{obj}$ but it seems unlikely that this will be necessary.

Note that the SED doesn't enter into the pixel-dependent part, C^r_{raw}, making it relatively simple to adopt a different SED and recalculate C_{std} if we know the $c^r_{\rm SED}$. We don't need to save $c^r_{\rm SED}$ for every object as we only need the SED, and that is known given $(\{C_b\}, \theta)$. This simplification depends on our assumption about the constancy of $\mathcal{S}^{tel}_{obj}/\mathcal{S}^{tel}_{sky}$ and $\mathcal{S}^{qe}_{obj}/\mathcal{S}^{qe}_{sky}$ over the object.

6.3 Colour Gradients

Because we using a model-based approach to handle SED dependencies we can easily handle more complicated problems; for example, if we are using a bulge/disk decomposition we are estimating the colours of each component, and can handle their SEDs separately when fitting our model.

A The Collimated Projector

A source of monochromatic light, driven by a light source equivalent to that used to illuminate the flatfield screen, capable of projecting an image mask (*e.g.* a set of spots) onto the focal plane. If we consider a mask with a single aperture the output is a parallel light with diameter equal to the diameter of the projector's exit pupil. This beam illuminates a small patch on the LSST's

What	Symbol	Nominal	Notes
Radial extent of M1		1.8m	$4.2m - 2.4m$
Number of bands	N_b	6	
Total LSST bandwidth		700nm	
Fraction of bandwidth scanned for each filter	$f_{\rm bandwidth}$	0.5	
Diameter of spot projector	$D_{\rm spot}$	0.3m	
Oversampling of M1	f_D	2	$f_D = 88$ to tile M1
Step in λ for spots (with a filter)	Δ_λ	$1_{\rm nm}$	
Step in λ for spots (without a filter)	$\Delta_{\lambda,\rm white}$	$10_{\rm nm}$	
Step in λ when measuring mask throughput	$\Delta_{\lambda,\rm hole}$	$100_{\rm nm}$	
Step in λ for flats (without a filter)	$\Delta_{\lambda,\rm flat}$	$100_{\rm nm}$	
Number of spots per CCD	$N_{\rm CCD}$	5	
Number of offsets to solve for hole sizes	$N_{\rm offset}$	9	can use one of spectral scans; total 10
Number of samples/filter for contamination check	$N_{\lambda/\rm filter}$	2	
Number of exposures per flat	$N_{\rm flat}$	10	per-pixel S/N ~ 1000
Elapsed time per set of flat data	$t_{\rm flat}$	$13_{\rm s}$	10s exposure
Elapsed time per set of spot data	$t_{\rm spot}$	$45_{\rm s}$	Assume 4s overhead, 15s exposure, and *c.* 26s overhead to move telescope/projector

Table 1: Parameters involved in defining calibration sequences

primary mirror, and is focused as a spot on the focal plane. For a 30cm aperture projector the area illuminated is *c.* 0.2%; the beam diameter is *c.* 20% of the annular radius of M1.

By using diffraction limited optics and a 10cm projector we can generate a beam with a divergence of *c.* 1 arcsec, which is then imaged into a 1 arcsec spot by the LSST optics; a larger projector could generate *c.* pixel-sized spots, allowing us to investigate PSF effects that were not resolved before the camera is fully assembled. When used for its primary photometric purpose we expect to generate *c.* 50-pixel spots.

In reality we can generate a number of spots simultaneously by putting an image mask in the projector's focal plane. The projector's output beam then diverges at 3.5°, illuminating an area with diameter *c.* 60cm; each focused spot still only illuminates a patch the size of the exit pupil of course. We may not assume that each spot is equally bright; not only are the holes in the image mask not going to be all identical, but the projector illumination is expected to vary slightly across the mask.

In addition to the direct image the projector will generate a series of ghosts, which form a set of distorted images of the pupil. Because the projector beam only illuminates a small portion of the primary, the projector ghosts are proportionally smaller than the full-pupil ghosts.

B Proposed Calibration Exposures

Nominal values for parameters such as the spot projector diameter, wavelength steps, and exposure times are given in Table 1. This table does *not* include filter change times, which there need to be added and should add at most 10–15 minutes per day (not trivial).

Let us initially assume that at all times we know the filter bandpasses $\mathcal{S}_b(\lambda, \boldsymbol{x})$ as a function

Activity	Interval day	Type	N/interval	N/year	t/interval hour	t/year hour	Scaling
contamination	1	F	120	43800	0.43	158	$\left(\frac{N_b}{6}\right)\left(\frac{N_{\lambda/\mathrm{filter}}}{2}\right)\left(\frac{N_{\mathrm{flat}}}{10}\right)$
bias	1	F	10	3650	0.01	2	
dark	7	F	3	156	0.84	44	$\left(\frac{t_{\mathrm{dark}}}{1000\mathrm{s}}\right)$
per-pixel flatfield	30	F	70	851	0.25	3	$\left(\frac{\Delta_{\lambda,\mathrm{flat}}}{100\mathrm{nm}}\right)\left(\frac{N_{\mathrm{flat}}}{10}\right)$
system throughput	30	S	840	10220	10.50	128	$\left(\frac{D_{\mathrm{spot}}}{0.3\mathrm{m}}\right)\left(\frac{f_D}{2}\right)\left(\frac{\Delta_{\lambda,\mathrm{white}}}{10\mathrm{nm}}\right)$
mask illumination	30	S	63	766	0.79	10	$\left(\frac{\Delta_{\lambda,\mathrm{hole}}}{100\mathrm{nm}}\right)\left(\frac{N_{\mathrm{offset}}}{9}\right)$
fringe flat	365	F	84000	84000	303.33	303	$\left(\frac{D_{\mathrm{spot}}}{0.3\mathrm{m}}\right)\left(\frac{f_D}{2}\right)\left(\frac{\Delta_{\lambda}}{1\mathrm{nm}}\right)\left(\frac{N_{\mathrm{flat}}}{10}\right)$

Table 2: Number of exposures needed to accomplish various tasks once we know $qe_n(\boldsymbol{x}, \lambda)$. The 'Types' are *F*lat and *S*pot. Per year, we need a total of 143444 exposures (648 hours), or an average of 392 exposures per day (1.77 hours). *N.b.* only the 'calibration' exposures are taken with a filter in the beam.

of position on the filter and wavelength. We'll consider whether we will be able to measure the bandpasses using the flat fields and spot projector in Section B.2.

B.1 Required Number of Exposures

The number of exposures and elapsed time resulting from the considerations in this section are given in Table 2; each of these exposures will result in a full camera read (6.4 Gby uncompressed).

We need 6 $\left(\frac{D_{\mathrm{spot}}}{0.3\mathrm{m}}\right)$ exposures to synthesize the full angular distribution of rays traversing the system using minimal overlaps on M1; let as adopt a number $6f_D$ with a nominal value $f_D = 2$. The spots on M1 should be placed at a range of azimuthal angles, and that we will monitor the sensitivity of derived calibration products to the positions of the spots, increasing f_D as appropriate.

Because we know $\mathcal{S}_b(\lambda, \boldsymbol{x})$ we can take exposures *without* any filter, so to cover the full spectral range we need 70 $\left(\frac{\Delta_{\lambda,\mathrm{white}}}{10\mathrm{nm}}\right)$ exposures.

We also need a spatial model of the sensitivity. If all the spots had the same brightness we could use the data taken to study the spectral response to model the (smoothly-varying) spatial structure. As each of these exposures includes 945 $\left(\frac{N_{\mathrm{CCD}}}{5}\right)$ spots this should be sufficient to map the expected smooth variation of the monochromatic throughput (*e.g.* we could use radial basis functions or expand to *c.* 45^{th} order Zernikes). In theory we only need perform this test at a single wavelength, but it seems prudent to check for wavelength-dependent effects in the projector (*e.g.* chromatic effects in the projector optics, diffraction moving light outside our measurement apertures).

If the CCDs show spatial features with significant wavelength dependencies (*e.g.* features in the anti-reflection coatings) we may need to increase N_{offset} for at least some wavelengths. The current test plan at BNL (Gilmore 2015) asks the vendors for QE measurements at 5 positions per CCD and this will probably suffice. We do not include an estimate of the cost of this possibility in Table 2.

In fact, as discussed in section 2.3, the illumination and sizes of all the holes in the mask won't be identical and we will need to take a number of exposures with different mask offsets and then solve for the intensity of each spot and the size of each hole. A detailed study of the number of

offsets, $N_{\rm offset}$ needed is *T.B.D.*; we shall adopt a nominal value of 9 (we can also reuse one of the exposures from the spectral scans). Because the study need not be repeated at more than one projector position the total calibration time is insensitive to the value of $N_{\rm offset}$.

We also need to know the small-scale variability of the response, primarily due to pixel effects. These are not expected to show strong spectral features, and may be measured using the flat field screen at a relatively coarse wavelength resolution. It is not easy to think of pixel-scale effects that evolve, but this data set may also be used to monitor the non-azimuthally symmetrical evolution of the system.

What can evolve is structures on the filters (although dust motes are far smaller than the beam size at the filter). We can monitor contamination with a single flat field taken at the central wavelength, but we allow for taking a small number of flat fields per filter.

These exposures may also be used to monitor the gain, although better measurements may be obtained using cosmic rays in science and dark exposures.

While taking flats we may as well also take bias and dark measurements (although these could also be taken on dark and stormy nights).

Finally, we need to know the fringe frames (especially in the y-band). We care about fringing in two ways: it produces small-scale structure in the sky, and it produces small-scale modulation in the throughput. It is possible that the former will be best measured from the sky, but the latter should be measured directly. Once again we can use unfiltered light, but need to scan at 1nm resolution. This is expensive. In reality we can probably relax this requirement. In the blue there are very few bright lines to worry about, and the chips are thicker in units of wavelength. Because fringes cover many pixels we can probably use data with lower S/N per pixel (recovering the fine structure from the regular flats); together these approaches are worth at least a factor of two, and probably five.

B.1.1 Frequency of Measurements

Please refer to Table 2 for the exposure times.

Not all these measurements need to be made at a common cadence. Because of the possibility of contamination we need to measure the per-pixel with-filter flats frequently; we say 'daily' in Table 2 but weekly would probably be sufficient (or possibly whenever we change filters). These are the only calibration exposures that need filters, and are therefore the only exposures that need pay the cost of filter changes.

The cost of the no-filter flat fields is comparable, but monthly scans should be good enough as it is hard to think of effects that vary even that fast.

The dark exposures are put in at a weekly cadence, but they are expected to vary only slowly if at all; the bias exposures are cheap and monitor changes in the noise properties of the amplifiers so we may as well take them daily.

The system throughput, like the no-filter flat fields, would be expected to vary only slowly, and we propose that they be taken at the same cadence, monthly. Note that we could take a subset more often. Whenever we take spot-projector flats we should also measure the mask illumination, but this is relatively cheap.

Finally, the fringes are not expected to vary as they are defined by the silicon; we conservatively take a set of fringe frames every year, but expect that this could be relaxed. Unfortunately doing so does not diminish the needed calibration in the first year unless the camera team delivers the required fringe data.

B.2 The Filter Transmission

One option for measuring the filter transmissions as a function of position is to build a machine that passes an f/1.2 beam through the filter and into a spectrophotometer; if the beam diameter is *c.* 10cm this directly measures the transmission as seen by the camera at that point in the filter, and we only need *c.* 50 exposures to fully characterise the system.

In the absence of such a machine, the spot projector can be used to monitor or measure the filter throughput. The area of the filter illuminated is about 2.1% $\left(\frac{N_{\rm CCD}}{5}\right)$, and we need *c.* 2520 $\left(\frac{D_{\rm spot}}{0.3{\rm m}}\right)\left(\frac{f_D}{2}\right)\left(\frac{\Delta_\lambda}{1{\rm nm}}\right)\left(\frac{N_b}{6}\right)\left(\frac{f_{\rm bandwidth}}{0.5}\right)$ exposures to cover the full spectral range; 31.5 hours. To explore all positions on the filter would take 1470 hours with 10s flats.

If we assume that the non-filter part of the transmission has no azimuthal symmetry, then these estimates must be increased by a factor of *c.* 45 and a full exploration would be prohibitively expensive.

It seems likely that we can use at least ten times as many spots without causing significant confusion due to ghosting, in which case each pointing of the collimated exposure illuminates *c.* 20% of the filter and we gain a factor of 10, so around 150 hours of integration. If we're willing to make stronger assumptions about the spatial coherence of the evolution of the filters we can obviously use fewer exposures. For example, if we assume that the properties of the filter don't vary significantly on the scale of the 10cm disk illuminated by M1, the 31.5 hour number quoted above is sufficient.

C Science Requirements Document (SRD)

The SRD specifications are:

Repeatability
: the median value of the photometric scatter for each star (the rms of calibrated magnitude measurements around the mean calibrated magnitude) shall not exceed 5 millimags in gri, 7.5 millimags in uzy. No more than 10% of these objects should have a photometric scatter larger than 15 mmag in gri, 22.5 mmag in uzy. This requirement sets the level above which we can reliably detect intrinsic variability in a single source.

Uniformity
: the rms of the internal photometric zeropoint error (for each visit) shall not exceed 10 millimags in grizy, 20 millimags in uzy. No more than 10% of these sources can be more than 15 mmag in gri or 22.5 mmag in uzy from the mean internal zeropoint. This places a constraint on the stability of the photometric system across the sky as well as an upper limit on various systematic uncertainties, such as any correlation of photometric calibration with varying stellar populations (or colors). This makes the photometry of sources directly comparable over the entire sky, and when combined with the previous requirement, creates a stable photometric system across the sky and over time, in a single filter.

Band-to-band photometric calibration
: The absolute band-to-band zeropoint calibration for main sequence stars must be known with an rms accuracy of 5 millimags for any color not involving u band, 10 millimags for colors constructed with u band photometry. This requirement ties photometric measurements in different filters together, enabling precise measurement of colors, and allows LSST photometry to be compared with that from other optical telescopes, and with astrophysical models.

Absolute photometric calibration
: The LSST photometric system must transform to an external physical scale (*e.g.* AB mags) with an rms accuracy of 10 millimags. This is essential for comparing with photometry from other wavelength regions, such as IR or UV.

D Glossary

$\mathcal{A}$
: The part of $\mathcal{F}$ that is due to scattered light and ghosting, *i.e.* is not proportional to the effective quantum efficiency of the detector.

BDRF
: Bi-Directional Reflection Function; the reflectivity of a surface in *this* direction in response to incident light from *that* direction.

DN
: Data Number; the value of a pixel as read from the detector (also called ADU)

$\mathcal{F}$
: The image of the flatfield screen in the b band (*i.e.* the data resulting from illumination of the camera with $\mathcal{I}$).

ISR
: Instrumental Signature Removal (remove bias, flatfield, *etc.*)

$\mathcal{I}$
: The illumination of the focal plane due to the flatfield screen; the light intensity just above the front surface of the detectors in the absence of telescope and filter effects.

i
: The pattern of non-uniform illumination of the focal plane in the absense of any telescope or camera effects except for the effects of vignetting (but corrected for the geometrical part of the vignetting — that is, the fraction of the pupil visible from a point in the focal plane).

QE
: Quantum Efficiency

$P_b^\ell(\lambda, \boldsymbol{x}_i, \boldsymbol{X})$
: The total flux in the primary image of the ℓ^{th} Stubbs Spot imaged through the b filter in a narrow range around wavelength λ at the point $\boldsymbol{x}_i$.

$\mathcal{S}$
: The effective quantum efficiency of a pixel.

  $\mathcal{S}^{tel}(\lambda, \boldsymbol{i})$ The probability of a photon incident on the pupil reaching the detector (neglecting vignetting and the filter)

  $\mathcal{S}_b^{filt}(\lambda, \boldsymbol{i})$ The probability that filter b transmits a photon

  $\mathcal{S}^{qe}(\lambda, \boldsymbol{i})$ The probability of a photon incident on the detector being detected

  $\mathcal{S}^{vig}(\lambda, \boldsymbol{i})$ The probability that a photon incident on the pupil will not be vignetted

  $\mathcal{S}^{optics}(\lambda, \boldsymbol{i})$ The effective area of a pixel (in units of nominal pixels) allowing for distortions

$\mathcal{S}^{ccd}(\lambda, \boldsymbol{i})$ The effective area of a pixel (in units of nominal pixels) allowing for physical changes in the size of the pixel (*e.g.* 'ragged gates').

S^{atm}
: The probability that a photon will pass through the atmosphere for a given visit.

S_b^{sys}
: The probability that a photon will pass through the telescope and camera (with the b filter) and be absorbed by the detector; assumed to vary relatively slowly with time.

$S_{b,std}$
: The probability that a photon incident on the atmosphere will be detected under 'standard' conditions; all photometry is referred to this probability.

SED
: Spectral Energy Distribution

S/N
: Signal-to-noise ratio

SRD
: Science Requirements Document

TBD
: The meaning of this acronym is To Be Decided

$\boldsymbol{x}$
: Coordinates in the focal plane. A function defined at a point is written $f(\boldsymbol{x}_i)$, whereas a function defined at all pixels is written $f(\boldsymbol{i})$.

$\boldsymbol{X}$
: Coordinates in the pupil.

References

Gilmore, K. (2015). *LSST Sensor Integrated Test Plan*. personal communication.

Jones, R. L. et al. (2013). *Level 2 Photometric Calibration for the LSST Survey*. URL: `http://ls.st/LSE-180` (visited on 07/14/2015).

Rasmussen, A (2015). *Sensor Modeling for the LSST Camera Focal Plane: Current Status of SLAC Originated Code*. URL: `http://ls.st/document-8590` (visited on 07/17/2015).